How to cite: *Angew. Chem. Int. Ed.* **2023,** *62,* e202217725
International Edition: doi.org/10.1002/anie.202217725
German Edition: doi.org/10.1002/ange.202217725

Host-Guest Interactions

Probing a Hydrogen-π Interaction Involving a Trapped Water Molecule in the Solid State

*Ettore Bartalucci[+], Alexander A. Malär[+], Anne Mehnert[+], Julius B. Kleine Büning, Lennart Günzel, Maik Icker, Martin Börner, Christian Wiebeler, Beat H. Meier, Stefan Grimme, Berthold Kersting, and Thomas Wiegand**

Abstract: The detection and characterization of trapped water molecules in chemical entities and biomacromolecules remains a challenging task for solid materials. We herein present proton-detected solid-state Nuclear Magnetic Resonance (NMR) experiments at 100 kHz magic-angle spinning and at high static magnetic-field strengths (28.2 T) enabling the detection of a single water molecule fixed in the calix[4]arene cavity of a lanthanide complex by a combination of three types of non-covalent interactions. The water proton resonances are detected at a chemical-shift value close to zero ppm, which we further confirm by quantum-chemical calculations. Density Functional Theory calculations pinpoint to the sensitivity of the proton chemical-shift value for hydrogen-π interactions. Our study highlights how proton-detected solid-state NMR is turning into the method-of-choice in probing weak non-covalent interactions driving a whole branch of molecular-recognition events in chemistry and biology.

Introduction

Water plays an essential role in a variety of chemical and biological processes. Many biological functions, including proton and electron transfer reactions in biological channels, protein activity and dynamics,[1] protein folding and structure,[2–4] as well as cell activity are governed by individual water molecules,[5] sometimes even involving entire water clusters.[6] For instance, water molecules have been reported to function in dimeric hemoglobin as allosteric mediators,[1] to mediate protein-ligand recognition in trypsin complexes[7] and to stabilize protein-protein interactions.[8] Crystalline water hydrates are furthermore of importance in pharmaceutical compounds and have been reported in templating nanoporous materials.[6]

The importance of water is particularly related to its capability of forming hydrogen bonds, typically between an electronegative element (e.g. N and O) and a hydrogen atom.[9] However, the definition of a hydrogen bond is not only limited to these cases.[10] For instance, also π-hydrogen bonds between delocalized π-electron clouds of aromatic rings and N, O and C-bound hydrogen atoms have been reported[11] and observed in biomolecules.[12] Such hydrogen bonds were classified as weak hydrogen bonds with bond energies less than 4 kcal mol^{-1} [6,9] and the water molecule features unusually short O–H bond lengths.[6] They poten-

[*] E. Bartalucci,[+] T. Wiegand
Max-Planck-Institute for Chemical Energy Conversion
Stiftstr. 34–36, 45470 Mülheim an der Ruhr (Germany)
E-mail: thomas.wiegand@cec.mpg.de

E. Bartalucci,[+] T. Wiegand
Institute of Technical and Macromolecular Chemistry, RWTH Aachen University
Worringerweg 2, 52074 Aachen (Germany)

A. A. Malär,[+] B. H. Meier
Physical Chemistry, ETH Zurich
8093 Zurich (Switzerland)

A. Mehnert,[+] L. Günzel, M. Börner, B. Kersting
Institute of Inorganic Chemistry, Leipzig University
Johannisallee 29, 04103 Leipzig (Germany)

J. B. Kleine Büning, S. Grimme
Mulliken Center for Theoretical Chemistry, Clausius Institute of Physical and Theoretical Chemistry, University of Bonn
Beringstraße 4, 53115 Bonn (Germany)

M. Icker
Institute of Organic Chemistry, Leipzig University
Linnéstraße 3, 04103 Leipzig (Germany)

C. Wiebeler
Institute of Analytic Chemistry, Leipzig University
Linnéstraße 3, 04103 Leipzig (Germany)
and
Wilhelm-Ostwald-Institute for Physical and Theoretical Chemistry, Leipzig University
Linnéstraße 2, 04103 Leipzig (Germany)

T. Wiegand
previous address: Physical Chemistry, ETH Zurich
8093 Zurich (Switzerland)

[+] These authors contributed equally to this work.

tially play an important role at hydrated biological surfaces.[13] From the chemical perspective, hydrogen-π bonds between aromatic rings and a water molecule[14] have for instance been observed by X-ray crystallography in calix[4]arene units which comprise a hydrophobic cavity that in the absence of hydrophobic guest molecules is occupied by a water molecule[15] as well as by single crystal neutron diffraction.[6] A network of water molecules has been reported in the structures of a variety of calix[n]arenes.[6,16]

Accurate refinement of water molecules is challenging by X-ray diffraction methods due to the well-known low scattering factor of hydrogen atoms. However, single-crystal neutron diffraction has been employed revealing the exact location of water molecules.[6] Proton-detected NMR spectroscopy is another major technique capable of directly detecting water molecules in chemical and biological contexts, particularly benefitting from the sensitivity of the proton chemical shift on the chemical environment as well as on the hydrogen bond strength.[17] This allows for probing water molecules engaged in hydrogen bonding, leading to more deshielded resonances. Protons engaged in π-hydrogen bond interactions and therefore above an aromatic plane, in contrast, are expected to resonate at lower frequencies (more shielded), which is caused by the circulating electron cloud in aromatic units (ring-current effects).[18] Aromaticity is for instance defined based on quantum-chemically calculated nucleus independent chemical-shift values,[19,20] also established in the solid state.[21] The development of fast magic-angle spinning (MAS) technology, typically achieving sample rotation frequencies of 110 kHz (or even 150–170 kHz[22,23]) provide nowadays sufficient resolution for the investigation of proton-detected spectra also in the solid state, mostly applied to biomacromolecules (for a recent review see ref. [24]), but for instance also applied to pharmaceutics (for selected examples see[25–27] which was in previous decades a domain reserved to solution-state NMR only. In addition to fast MAS, an approach revealing pure isotropic proton solid-state NMR spectra has been reported.[28] Proton-detected solid-state NMR at slower MAS frequencies (<35 kHz) has already been successfully employed in probing supramolecular host-guest interactions,[29,30] for instance by detecting the low-frequency shifted ^{1}H resonances of guest molecules (toluene and pyridine) in *p-tert*-butylcalix[4]arene complexes enabling structure determination by "NMR crystallography".[30,31]

We herein report a novel vanillylimine-appended calix[4]arene La^{3+}/K^{+} complex which hosts a single water molecule within the calix[4]arene cavity by a combination of three types of non-covalent interactions, making it a suitable target for exploring recent advances in the field of solid-state NMR to study such interactions. Solid-state NMR experiments at 100 kHz MAS frequency allow not only for the spectroscopic characterization of the trapped water molecule, but enable as well a full structural investigation of the complex. The high magnetic-field strength employed (28.2 T corresponding to 1200 MHz proton Larmor frequency[32]) avoids the requirement of any specific isotope labelling and an assignment of the NMR resonances by proton-detected ^{13}C,^{1}H heteronuclear correlation experiments becomes possible, including the spectroscopic identification of the trapped water signals. Density Functional Theory (DFT) calculations support the resonance assignments. The unusual, strongly shielded resonances of the water protons indeed point to the capture of an isolated water molecule. DFT calculations were performed as well to further unravel the role of a hydrogen-π interaction on the observed proton chemical-shift values and reveal that a maximum shielding effect of around −1.5 ppm is possible for hydrogen-π interactions. Our solid-state NMR approaches are extendable to the detection of protons engaged in weak, non-covalent interactions, driving a whole branch of molecular-recognition events in chemistry and biology. A particularly important example comprises the nowadays intensively discussed area of liquid-liquid phase separation that seems to be governed by cation-π interactions highlighting the fundamental role of such interactions in biological processes.[33]

Results and Discussion

The vanillylimine-appended calix[4]arene, hereafter abbreviated as H_4L, was prepared according to a published procedure.[34] Treatment of the triethylammonium salt of H_4L with lanthanum(III) nitrate hexahydrate and potassium carbonate in a 1:1:1 molar ratio at room temperature in a mixed CH_2Cl_2/MeOH solution (1:1) reproducibly affords a pale-yellow solution, from which the pale-yellow neutral complex [K(H_2O)LaL] (compound **1**) precipitates in nearly quantitative yield (Scheme 1). The structure of the diamagnetic K^{+}/La^{3+} complex in solution was studied by mass spectrometry and one- and two-dimensional NMR spectroscopy in solution (see Figures S1–S10).

Pale-yellow single-crystals of [K(H_2O)LaL] (**1**) suitable for X-ray crystallographic analysis[35] were obtained from CH_2Cl_2-d_2 solutions that were used for the NMR studies (for the X-ray crystallographic characterization of the free ligand H_4L see Supporting Information and Figure S11 therein [36]). The crystal structure of **1** comprises neutral [K(H_2O)LaL] complexes, which are linked by intermolecular hydrogen bonding interactions (Figure 1). The potassium ion is located in the calix[4]arene cavity, being coordinated by two phenolate O atoms and two aryl rings from the calix[4]arene and one water molecule. The $K^{+}\cdots\eta^{6}$ arene (centroid) distances at 2.94 Å and 2.97 Å differ slightly, but lie in a typical range for $K^{+}\cdots\pi$ interactions.[37,38] The open coordination site of the K^{+} ion is shielded by a vanillin ring of an adjacent complex. This intermolecular $K^{+}\cdots\eta^{6}$ arene (centroid) distance of 4.36 Å, however, is rather long and suggests that the π-system of this ring does not interact with the K^{+} ion. The single H_2O molecule in **1** appears to be involved in three non-covalent interactions. The $K^{+}\cdots OH_2$ interaction can be considered as an electrostatic "ion-dipole" interaction and its distance (2.71 Å) is typical for eight-coordinated K^{+} aqua complexes.[39,40] The water molecule is further involved in an intramolecular HOH···π interaction with one of the phenolate rings as suggested by the relatively short O···arene (centroid) distance of

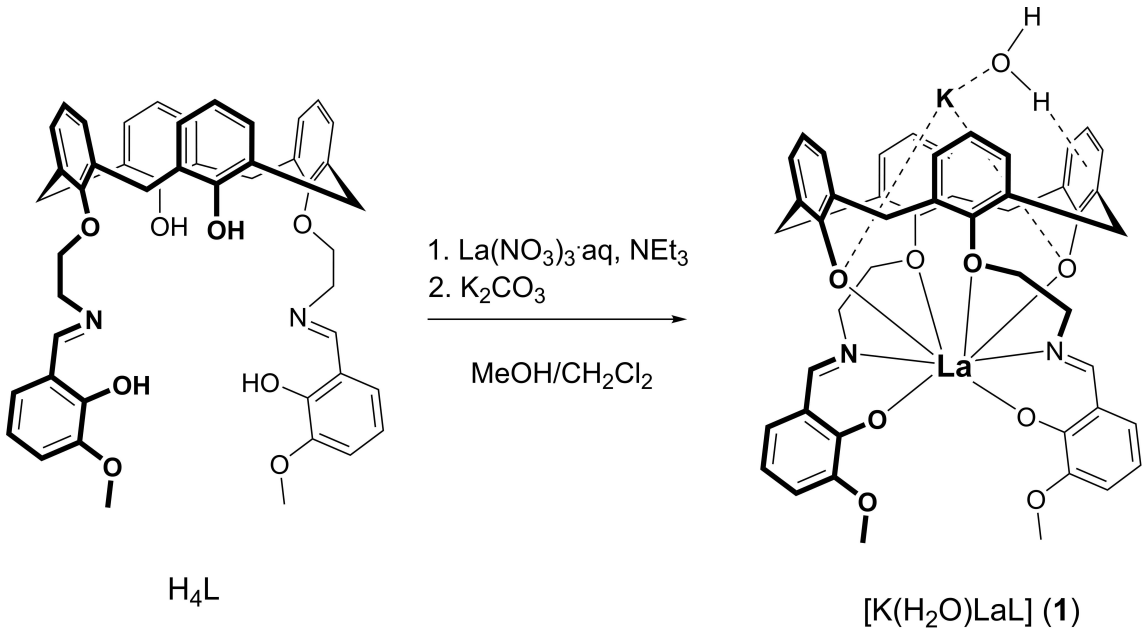

Scheme 1. Synthesis of the neutral La complex **1** starting from the vanillylimine-appended calix[4]arene H_4L.

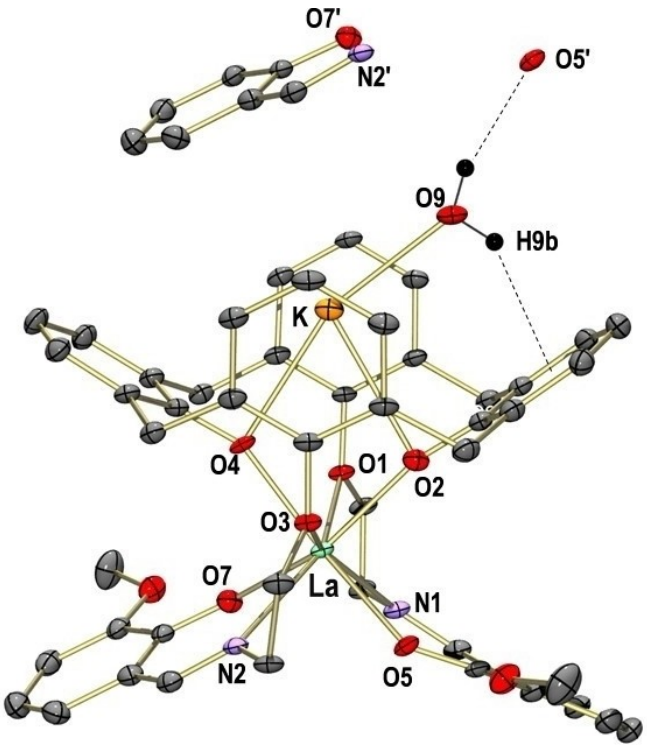

Figure 1. Molecular structure of the [K(H_2O)LaL] complex in the solid state (50% thermal ellipsoids). The H-atoms (except for H_2O) are omitted for clarity. Dashed lines refer to H_2O···π and HOH···O hydrogen bonding interactions. Selected distances in Å: La···O1 2.732(4), La···O2 2.336(4), La···O3 2.692(4), La···O4 2.349(4), La···O5 2.398(4), La···O7 2.360(4), La···N1 2.643(6), La···N2 2.672(5), K···O2 3.117(5), K···O4 2.801(4), K···O9 2.713(6), O9···O5′ 2.950(8), O1(arene)^{centroid}···O-(3)arene^{centroid} 5.8135(2). Symmetry code used to generate equivalent atoms: $1+x, y, z$ (′).

3.24 Å.[34,41] Thus, a value of 3.3 Å has been determined experimentally for the distance between the centre of mass of water and the $C_6H_6{\cdot}H_2O$ complex.[14] The water molecule forms also a weak intermolecular hydrogen bond with a La-bound aryloxide group of an adjacent complex (O9···O5′ 2.95 Å). Although both H atoms could be located from final Fourier maps, their exact positions remain elusive, due to the difficulties in localizing them accurately at the obtained resolution of the electron density.[42] The ATR FTIR spectrum of [K(H_2O)LaL] (Figure S12) reveals two OH stretching bands at 3574 cm^{-1} and 3400 cm^{-1}. These values are red shifted from those reported for isolated H_2O molecules as expected for the presence of hydrogen bonding interactions.[14] This trend is also qualitatively reproduced by vibrational frequency calculations at the semiempirical GFN2-xTB[43] level-of-theory using the single-point Hessian (SPH)[44] approach (see Supporting Information, e.g. Table S1, for more details). The La^{3+} ions are eight-coordinated by four calix[4]arene O atoms and two imine N and O atoms of the pendant vanillylimine Schiff base units. The coordination environment is best described as biaugmented trigonal prismatic as implied by a shape symmetry factor[45] of 4.13 (Table S2). The La–O and La–N distances are typical for coordination number 8, ranging from 2.33 to 2.73 Å.[46]

The ^{13}C NMR spectrum of **1** in solution (Figure 2a, blue) shows 14 signals for the calix[4]arene moiety and six signals for the two salicylidene fragments, which suggest time-averaged C_2 symmetry and/or fast exchange of K^+-bound co-ligands. C_2 symmetry could arise when the two open coordination sites of the K^+ ion are occupied by identical solvate molecules (L′ = H_2O) as illustrated in Scheme 2. Indeed, such K^+ coordination environments have been reported, as for example in the complex [K(L′)$_2$Ti(calix[4]arene)(acac)] with L′ = MeOH or THF.[47] The ^{13}C signal

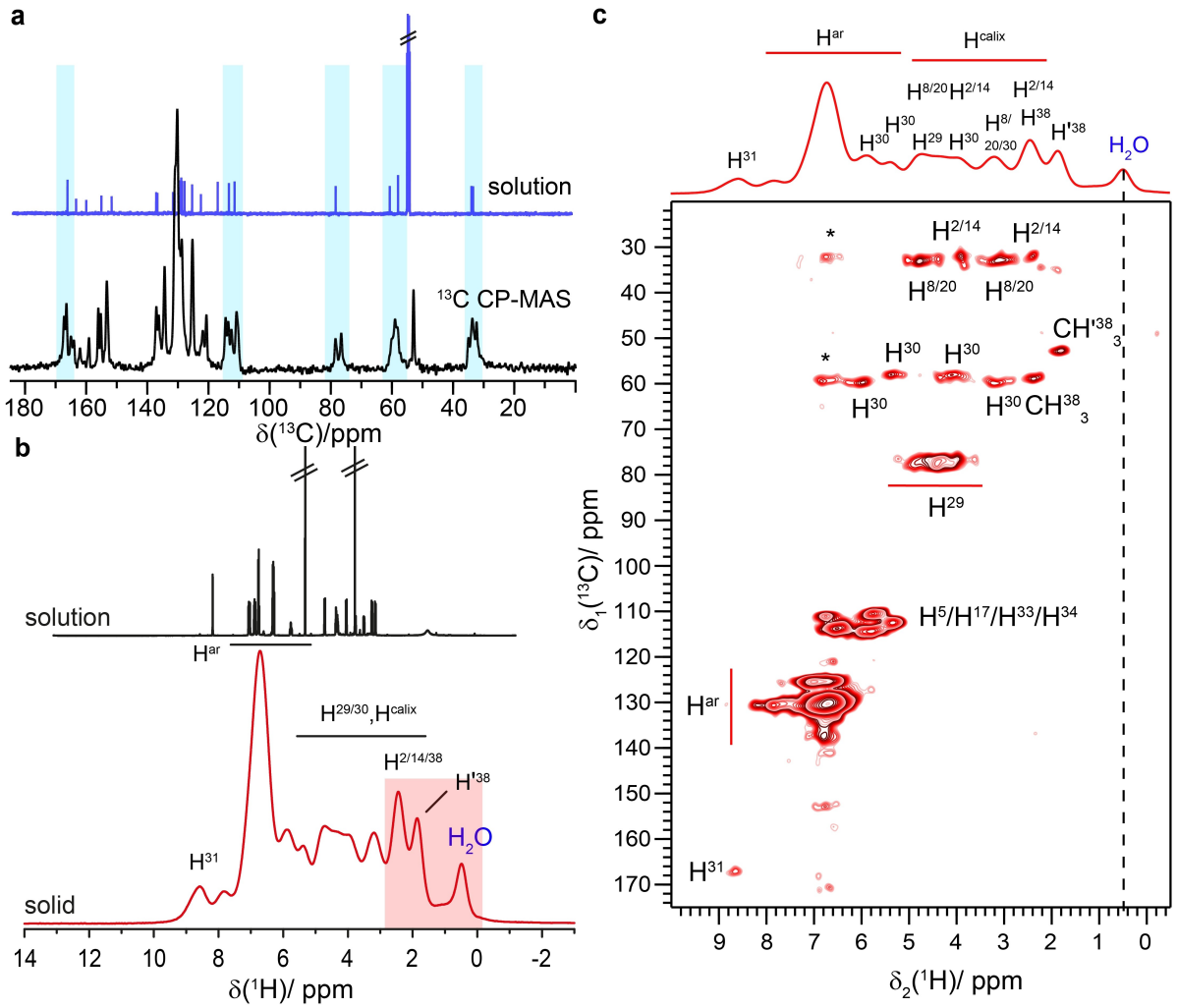

Figure 2. The spectroscopic characterization by NMR of **1** in the solid state is achieved employing fast MAS and a high static magnetic field. a) ^{13}C solution-state NMR spectrum recorded at 11.7 T (blue) and ^{13}C-detected ^{1}H,^{13}C CP-MAS solid-state NMR spectrum of **1** (black) recorded at 60 kHz MAS and 16.4 T. Blue-shaded spectral regions show peak doubling observed in the solid state. b) ^{1}H-detected MAS spectrum of **1** recorded at 100 kHz measured and 28.2 T. The top spectrum represents the solution-state NMR spectrum recorded at 11.7 T. Some resonance assignments (see below) are indicated on the spectrum. Resonances highlighted in red are absent in solution. c) *hCH correlation spectroscopy enables resonance assignment.* Natural abundance 2D-hCH correlation spectrum of **1** recorded at 100 kHz MAS and 28.2 T external magnetic-field strength. The lowest contour level is plotted at 2 times noise RMSD. The contour level increment is 1.1. The ^{1}H-MAS spectrum recorded under the same experimental conditions is displayed in red on top of the panel. Assignments have been obtained by comparison with the ^{13}C-detected solution-state spectrum from (a). For atom numbering, see Scheme 1. The vertical dashed line denotes the low-ppm proton chemical-shift position of the trapped water resonances. * indicate contacts between different C–H groups.

for C atoms bearing phenolic O atoms is known to depend strongly on the protonation state and environment,[48,49] ranging from limiting values of about 154 ppm for the neutral PhOH form to around 174 ppm for naked PhO^- anions (in CH_2Cl_2-d_2 solution). The chemical-shift values for the corresponding C atoms in **1** are detected at 160.7 ppm for the pendant vanillylimine groups and at 164.1 ppm for the calix[4]arene scaffold, respectively. These values deviate clearly from the value of 174 ppm seen for naked phenolate anions, providing further support for the fact that the aryloxide groups interact with the K^+ and La^{3+} ions. The ^{1}H NMR spectrum of **1** (Figure S13) also reveals a resonance at 1.4 ppm, which is assigned to free water in the solvent CD_2Cl_2.[50]

We next moved to solid-state NMR and recorded ^{13}C-detected ^{1}H,^{13}C cross-polarization (CP)-MAS experiments. The comparison of solution and solid-state NMR spectra is provided in Figure 2a. Interestingly, several ^{13}C resonances show a peak doubling not observed in solution, pointing to crystallographically distinct sites (highlighted in blue in Figure 2a). We thus attribute this effect to a structural inequivalence of the two vanillylimine Schiff base units and thus a break of the C_2 symmetry which is present in solution (as illustrated in Scheme 2). This is in agreement with the crystal structure in which the irregular coordination geometry about the K^+ ion (trapped water molecule) is responsible for the symmetry reduction (Figure 1).

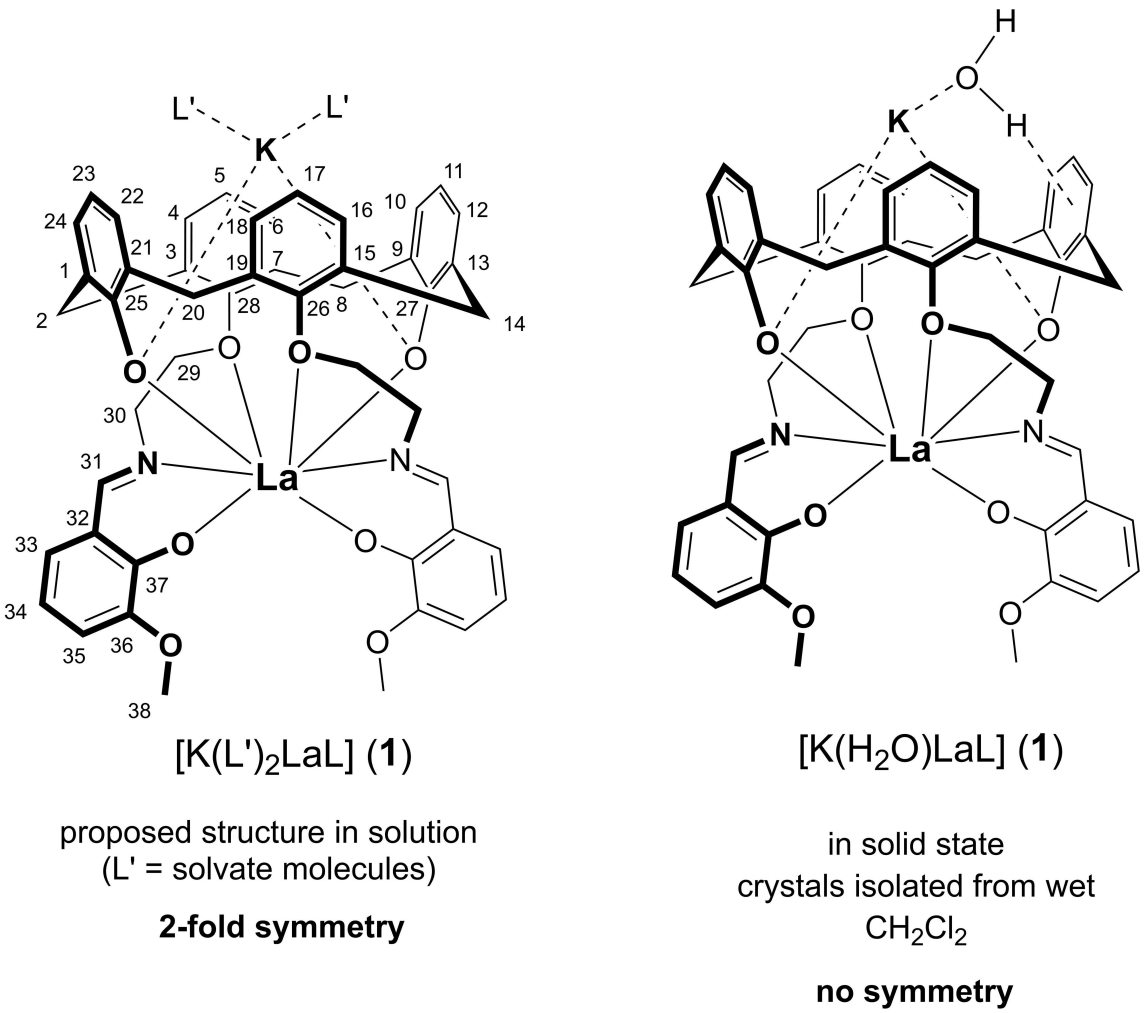

Scheme 2. Symmetry reduction of **1** upon going from the solution to the solid state. The atom numbering used herein is given on the left.

Proton-detected solid-state NMR at fast MAS frequencies should allow for a direct detection of the trapped water molecule, thus providing more insights into the bonding behaviour and extending our previous knowledge obtained from the X-ray structure. Figure 2b presents the ^{1}H-detected MAS spectra of **1** recorded at 100 kHz MAS at a magnetic field of 28.2 T using only sub-milligram sample amounts. We observe the expected increase in spectral resolution with increasing MAS frequency as reported in biological and chemical contexts due to a more efficient reduction of residual homonuclear proton dipolar coupling-induced broadening at faster MAS[24,51,52] (see Figure S13 and S14). The homogeneous broadening at 1200 MHz is smaller than at 850 MHz for most resonances (Figure S14) highlighting the advantage of high steady-state magnetic fields.

Overall spectral resolution is higher at 1200 MHz compared to 850 MHz (see Figure S15 for a comparison with the spectrum at 850 MHz), despite the fact that the proton linewidths in **1** are significantly affected by inhomogeneous broadening effects, either caused by structural heterogeneities (e.g. slight structural perturbations in the aromatic units) or anisotropic bulk magnetic susceptibility effects.[53–56] Note, that additional spectral overlap in such spectra arises from the crystallographic inequivalence of the two vanillylimine Schiff base units and the local C_2 symmetry break induced by the trapped water molecule (see above), making **1** a particularly challenging target for solid-state NMR. Interestingly, the solid-state NMR spectrum shows additional resonances at low ppm-values (0.4, 1.8 and 2.4 ppm) that remain absent in solution (highlighted in red in Figure 2b). At this point we speculate that at least one of the additional resonances appearing in the solid-state NMR spectrum at low frequencies might be assigned to the water molecule trapped in the calixarene moiety that has been observed crystallographically (see Figure 1). Water chemical-shift values around 0 ppm have been described for isolated water proton resonances in the gas phase, whereas liquid water resonates at significantly higher chemical-shift values (around 4.8 ppm).[57,58] Strongly low-frequency shifted proton water resonances have already been detected in the solid state for instance for water molecules sorbed on carbonaceous materials.[59–61]

For identifying which of the proton resonances belong to the trapped water molecule, we recorded a proton-detected

CP-based 2D hCH spectrum with short CP contact times. This experiment filters protons that do not possess a directly bound carbon atom. The availability of the high static magnetic field (1200 MHz) combined with fast MAS (100 kHz) allowed for recording such a spectrum in only 22 hours using sub-milligram amounts of non-isotopically labelled sample. Figure 2c shows the hCH spectrum and the obtained resonance assignments using previously assigned ^{13}C solution-state NMR shifts for guidance (see Table 1). And indeed, the resonance at 0.4 ppm (marked with a vertical dashed line) remains absent in the spectrum supporting the assignment to the trapped water molecule. The same observation is made when comparing a 1D hcH spectrum to the ^{1}H-MAS spectrum, in which also the resonance at 0.4 ppm is missing (Figure S16). The other two resonances at low frequencies (1.8 and 2.4 ppm) which remain absent in the solution-state NMR spectra are assigned to the methyl groups (H'^{38}/H^{38}) and calixarene (H^{2}/H^{14}) protons. The observation of two methyl groups, both fast rotating on the NMR timescale, is supported by their crystallographic inequivalence illustrating that proton-detected solid-state NMR is very sensitive in detecting the small structural differences in the two vanillylimine Schiff base units. We have also recorded ^{13}C dipolar dephasing CP-MAS spectra in which CH and CH_2 groups are strongly attenuated (or even disappearing) in the spectra, whereas quaternary carbon atoms as well as methyl groups remain visible (see Figure S17, also for a comparison with the solution-state spectrum including resonance assignments). And indeed, the two methyl groups possess different ^{13}C chemical-shift values (53 and 59 ppm), further supporting the resonance assignments. Under the used experimental conditions, we are even able to distinguish the intra-methylene protons (e.g. H^{30}, H^{8}/H^{20} and H^{2}/H^{14}) revealing significant chemical-shift differences as also observed by solution-state NMR. The resonance at highest frequency (8.7 ppm) is assigned to the imino proton of the Schiff base.

We next recorded a 2D ^{1}H-^{1}H single-quantum (SQ)/double-quantum (DQ) correlation spectrum at 100 kHz MAS using the Back-to-Back (BaBa) recoupling sequence[62] with 80 μs mixing time to further support the assignment of the resonance at 0.4 ppm to a water molecule proton and elucidate the position of the second water proton resonance (Figure 3a). In the case were both water protons resonate close to 0.4 ppm (nearly degenerate chemical shifts), a correlation peak at the sum of the two chemical-shift values (0.8 ppm) in the indirect dimension should appear. And indeed, this is observed for the resonance at low-ppm values assigned to the water molecule. The water protons have thus, within the experimentally achieved linewidths, similar chemical-shift values. In addition, the peak intensity of the 0.4 ppm resonance is consistent with two protons, for instance by comparing it to the intensity of the imino protons at 8.7 ppm. The BaBa spectrum is further used to support the resonance assignments derived so far (see the blue dashed horizontal lines in Figure 3a revealing protons in close spatial proximity). Particularly, the chemically distinct protons of the methylene groups are clearly identified. In addition, we have recorded ^{1}H-^{1}H spin-diffusion (SD) based spectra with different mixing times (see Figure 3b for the spectrum with 100 ms mixing time, and Figure S18 for the spectra with 10 and 50 ms mixing time). Such spectra are often used for proton resonance assignment purposes,[63,64] although their interpretation remains challenging in the present case due to significant spectral overlap in the 2D spectra, the dependence of the spin-diffusion mechanism on the chemical-shift differences and the MAS frequency and their general lack in selectivity. However, the spectrum at long mixing times (Figures 3b) clearly reveals cross-peaks and thus spin diffusion for the water resonance at low-ppm values to further resonances of the lanthanide complexes, which is a clear evidence that we indeed detect a trapped water molecule. Interestingly, there are further cross-peaks observed for the low-intensity resonance at around 1.1 ppm, possibly a second water molecule trapped in the complex (marked by + in Figure 3b).

We also noticed several cross-peaks involving the methyl group protons with negative intensity in the ^{1}H-^{1}H spectra (e.g. opposite intensity than the diagonal), particularly intense at shorter mixing times (Figure S18), possibly originating from incoherent cross relaxation effects induced by the fast rotating methyl groups as observed in NOESY spectra[65] in case of short correlation times,[66] which needs to be further evaluated for the present case. Negative cross-peaks in spin-diffusion based spectra have also been reported originating from a coherent mechanism,[67] which also remains a possible explanation for the observed negative cross-peaks. Interestingly, the SD spectrum with the shortest mixing time of 10 ms (Figure S18) already reveals a contact between the water protons and a methyl group that can only be realized by an intermolecular contact, whereas short-range contacts to the aromatic protons remain unobserved, most likely due to an inefficient SD process caused by the large chemical-shift differences.[68]

To further support the assignment of the strongly shielded resonance to the bound water molecule, we turned to DFT calculations. For the complex **1** in vacuo, the most shielded protons obtained are those of the water molecule with −0.60 and 0.03 ppm at the PBE0/pcSseg-2 level-of-theory in reasonable agreement with the experimental value

Table 1: Comparison of solid and solution-state NMR proton chemical-shift values.

Proton species	$\delta^{solid}(^{1}H)$ [ppm]	$\delta^{solution}(^{1}H)$ [ppm]
H_2O	0.4	n.d.[a]
H'38/H38	1.8; 2.4	3.8
H30	3.2/6.0; 4.1/5.4	3.5/5.8
H29	4.3	4.4
H8/H20	3.1/4.8	3.3/4.7
H2/H14	2.4/3.9	3.2/4.1
H5/H17/H33/H34	5.3–6.8	6.3–6.8
H31	8.7	8.2

[a] The absence of the resonance in the solution-state NMR spectrum is possibly attributed to fast exchange with residual H_2O content in the CD_2Cl_2 solvent. For H38, two resolved resonances are detected caused by the crystallographic inequivalence of the two vanillylimine Schiff base units.

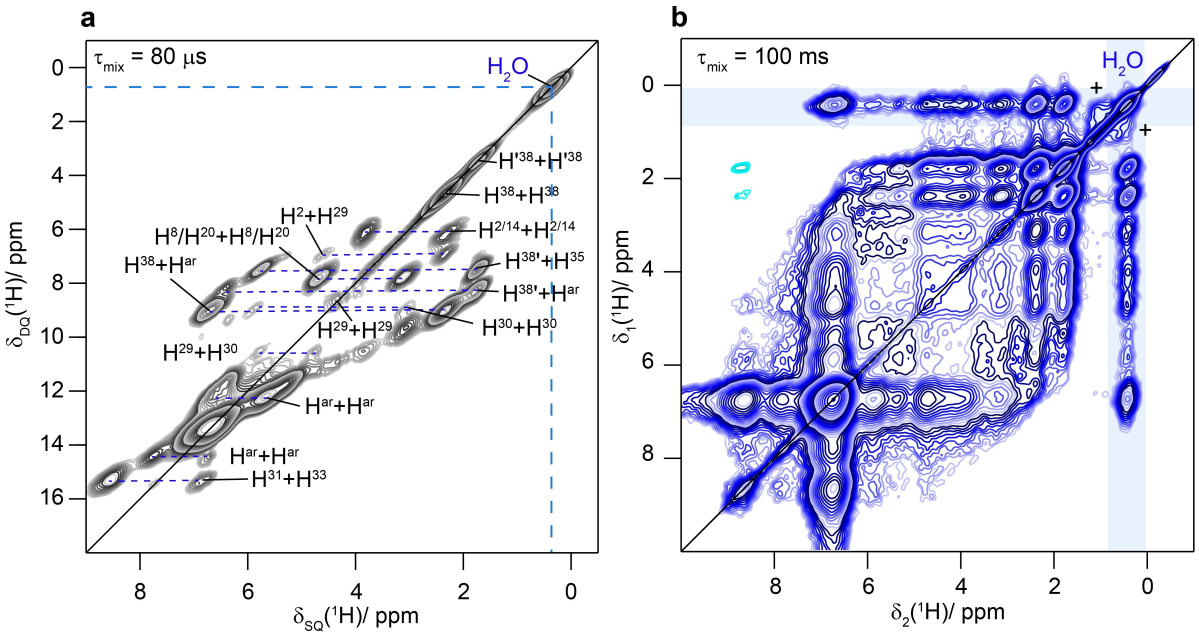

Figure 3. ^{1}H-^{1}H correlation spectroscopy reveals spatial proximities for the trapped water molecule. a) Single-quantum-double quantum ^{1}H-^{1}H spectrum of **1** employing BaBa recoupling with 80 µs mixing at 100 kHz MAS and 28.2 T. Spatial proximities are highlighted by horizontal blue-dashed lines. The black solid line denotes the double-quantum diagonal. The lowest contour level is plotted at 15 times noise RMSD. 64 contour levels with an increment of 1.1 are shown. b) ^{1}H-^{1}H spin diffusion-based spectrum of **1** recorded at 100 kHz MAS and 20.0 T with mixing times of 100 ms. The lowest contour level is plotted at 8 times noise RMSD. 64 contour levels with an increment of 1.1 are shown. The blue bands highlight correlation peaks encoding spatial proximity information for the trapped water. The cyan peaks represent negative contour levels. + indicates possibly a second water molecule trapped in the complex.

(0.4 ppm, see below). Compound **1** is a particularly suitable compound to further address the influence of the hydrogen-π interaction and therefore the aromatic ring-current effects on the water proton chemical-shift values. To disentangle the contribution of this interaction from other local effects on the magnetic shielding of the water protons, we performed calculations using a model extracted from the crystal structure comprising a water and a benzene molecule with relaxed positions of the hydrogen atoms (via a constraint optimization using the r^{2}SCAN-3c[69] composite density functional approximation). Figure 4 shows the distance dependence of the water proton chemical-shift values (given as the relative change with respect to the dissociation limit, Δδ) from the benzene plane as calculated at the PBE0/pcSseg-2[70,71] level-of-theory (which are confirmed by highly accurate coupled cluster CCSD(T)/TZ + extrap.[72–78] calculations; see the Supporting Information for these, Figure S19, and for further technical details). The curve of the proton facing the benzene plane (H_A) resembles a potential-energy curve with the maximal chemical-shift change of −1.9 ppm for the distance of 2.25 Å, which corresponds to the hydrogen-benzene distance in the crystal structure of compound **1**. The second water proton (H_B) exhibits a much smaller change in chemical shift at the measured distance, as it points away from the aromatic plane and is thus less exposed to the ring-current effects. This analysis clearly reveals that NMR itself is sensitive enough to probe the engagement of protons in such interactions, which is of particular relevance for instance in bio-macromolecules.[12] However, as mentioned above, the two water protons in **1** experimentally show rather similar chemical-shift values, which can be explained either by a still insufficient resolution in the solid-state NMR spectra or by chemical-exchange effects, e.g., a two-site jump of the H_2O molecule. In the latter case, the distance dependence is best described by the average of both chemical-shift values (gray curve in Figure 4), which still shows a maximum change of −1.65 ppm (at a slightly shorter distance of 2.03 Å), still significant enough for an experimental distinction between a (non-covalently) bound and an unbound state. The ^{1}H chemical-shift values of the benzene protons are much less sensitive to the water-benzene distance and thus to the hydrogen-π interaction (see Figure S20). Note that the experimentally-observed low-frequency shifts of the methyl groups (H38 and H′38) of compound **1** (1.8 and 2.4 ppm) are caused by intermolecular ring-current effects[20,21] as discussed in detail in the Supporting Information (see Figure S21).

Conclusion

In conclusion, we have presented the spectroscopic characterization of an isolated, trapped water molecule in a

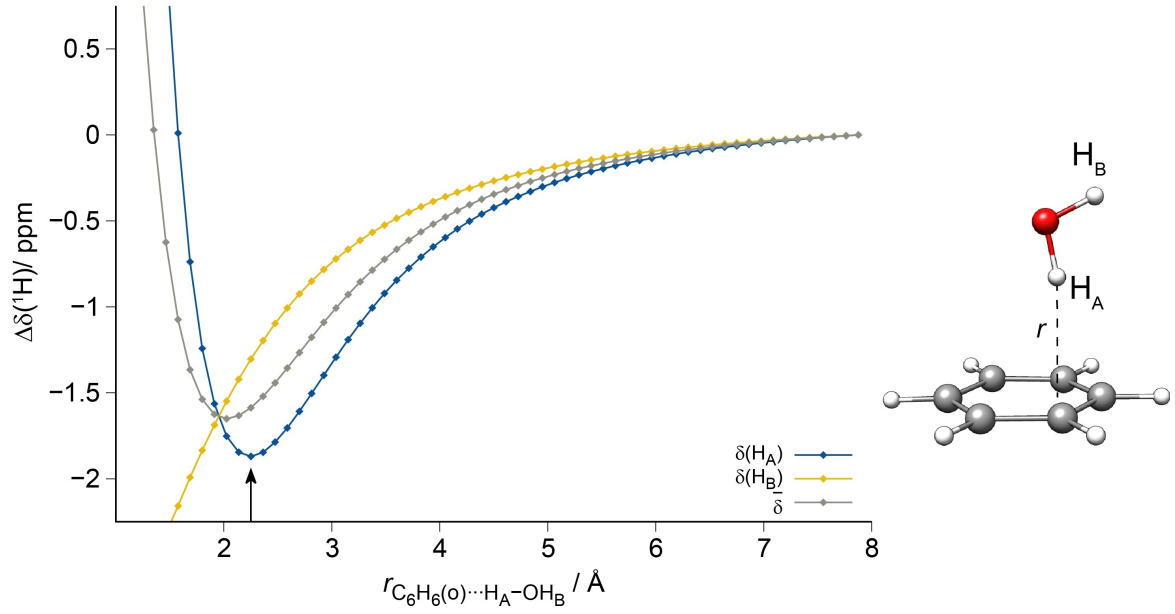

Figure 4. Proton NMR chemical-shift values are sensitive reporters for hydrogen-π interactions as revealed by quantum chemical calculations. Relative (with respect to the dissociation limit) ^{1}H NMR chemical shifts Δδ of a water molecule (protons H_A, H_B and their average value) as a function of its distance from a benzene molecule given as the projection of the H_A atom onto the aromatic plane. Calculations have been performed using the PBE0 density functional approximation with the pcSseg-2 basis set (see Supporting Information for details). The arrow indicates the distance found in the crystal structure of compound **1**.

calix[4]arene lanthanide complex by solid-state NMR. The combination of fast MAS with high steady-state magnetic fields have allowed us identifying the water proton resonances at rather unusual low-frequency chemical-shift values close to zero ppm, similar to reported gas phase water shifts. We have shown by DFT calculations that hydrogen-π interactions, which are an important molecular grammar in chemistry and biology, can lead to a further shielding of the proton resonances, depending significantly on the distance of the protons with respect to the aromatic plane. The reported lanthanide complex will serve as a model to further investigate hydrogen-π interactions, for instance to explore experimentally the distance-dependence of ^{1}H chemical-shift values by substituting the potassium ion with further alkali metal ions. Our study paves the way for further inspecting the sensitivity of NMR observables for probing the role of weak non-covalent interactions in transient molecular recognition events.

Acknowledgements

T.W. acknowledges support from the Deutsche Forschungsgemeinschaft (DFG, German Research Foundation, project number 455240421 and Heisenberg fellowship, project number 455238107) and the Max Planck society. T.W and E.B. thank MSc Sabrina Smid (RWTH Aachen University) for performing initial DFT calculations. B.H.M. acknowledges support by an ERC Advanced Grant (grant number 741863, Faster). J.B.K.B. is grateful for financial support by the "Fonds der Chemischen Industrie (FCI)". We are thankful to Prof. Dr. H. Krautscheid for providing facilities for X-ray crystallographic measurements. Financial support from the German Federal Ministry of Education and Research (BMBF—project 02NUK046C, B.K.) is gratefully acknowledged. C.W. thanks Prof. Dr. R. Tonner and Prof. Dr. J. Matysik (both University of Leipzig, Germany) for fruitful discussions and acknowledges the Leipzig University Computing Center for providing computing time. Open Access funding enabled and organized by Projekt DEAL.

Conflict of Interest

The authors declare no conflict of interest.

Data Availability Statement

Solid-state NMR raw data are available under the doi number 10.5281/zenodo.7520459.

Keywords: Calixarene · DFT · Hydrogen-π Interaction · Lanthanide · Solid-State NMR

[1] W. E. Royer, A. Pardanani, Q. H. Gibson, E. S. Peterson, J. M. Friedman, *Proc. Natl. Acad. Sci. USA* **1996**, *93*, 14526.
[2] M. M. Teeter, *Proc. Natl. Acad. Sci. USA* **1984**, *81*, 6014.
[3] E. N. Baker, *J. Mol. Biol.* **1980**, *141*, 441.
[4] Y. Levy, J. N. Onuchic, *Proc. Natl. Acad. Sci. USA* **2004**, *101*, 3325.
[5] M. Chaplin, *Nat. Rev. Mol. Cell Biol.* **2006**, *7*, 861.

[6] K. Fucke, K. M. Anderson, M. H. Filby, M. Henry, J. Wright, S. A. Mason, M. J. Gutmann, L. J. Barbour, C. Oliver, A. W. Coleman, J. L. Atwood, J. A. K. Howard, J. W. Steed, *Chem. Eur. J.* **2011**, *17*, 10259.

[7] J. Schiebel, R. Gaspari, T. Wulsdorf, K. Ngo, C. Sohn, T. E. Schrader, A. Cavalli, A. Ostermann, A. Heine, G. Klebe, *Nat. Commun.* **2018**, *9*, 3559.

[8] F. Rodier, R. P. Bahadur, P. Chakrabarti, J. Janin, *Proteins Struct. Funct. Bioinf.* **2005**, *60*, 36.

[9] G. A. Jeffrey, *An Introduction to Hydrogen Bonding*, Oxford University Press, Oxford, **1997**.

[10] T. Steiner, *Angew. Chem. Int. Ed.* **2002**, *41*, 48; *Angew. Chem.* **2002**, *114*, 50.

[11] T. S. Zwier, *Annu. Rev. Phys. Chem.* **1996**, *47*, 205.

[12] T. Steiner, G. Koellner, *J. Mol. Biol.* **2001**, *305*, 535.

[13] K. P. Gierszal, J. G. Davis, M. D. Hands, D. S. Wilcox, L. V. Slipchenko, D. Ben-Amotz, *J. Phys. Chem. Lett.* **2011**, *2*, 2930.

[14] S. Suzuki, P. G. Green, R. E. Bumgarner, S. Dasgupta, W. A. Goddard, G. A. Blake, *Science* **1992**, *257*, 942.

[15] J. L. Atwood, F. Hamada, K. D. Robinson, G. W. Orr, R. L. Vincent, *Nature* **1991**, *349*, 683.

[16] J. L. Atwood, L. J. Barbour, M. J. Hardie, C. L. Raston, *Coord. Chem. Rev.* **2001**, *222*, 3.

[17] G. Wagner, A. Pardi, K. Wuethrich, *J. Am. Chem. Soc.* **1983**, *105*, 5948.

[18] R. J. Anderson, T. P. McNicholas, A. Kleinhammes, A. Wang, J. Liu, Y. Wu, *J. Am. Chem. Soc.* **2010**, *132*, 8618.

[19] Z. Chen, C. S. Wannere, C. Corminboeuf, R. Puchta, P. v. R. Schleyer, *Chem. Rev.* **2005**, *105*, 3842.

[20] P. v. R. Schleyer, C. Maerker, A. Dransfeld, H. Jiao, N. J. R. van Eikema Hommes, *J. Am. Chem. Soc.* **1996**, *118*, 6317.

[21] M. Zilka, S. Sturniolo, S. P. Brown, J. R. Yates, *J. Chem. Phys.* **2017**, *147*, 144203.

[22] M. Schledorn, A. A. Malar, A. Torosyan, S. Penzel, D. Klose, A. Oss, M. L. Org, S. Wang, L. Lecoq, R. Cadalbert, A. Samoson, A. Bockmann, B. H. Meier, *ChemBioChem* **2020**, *21*, 2540.

[23] E. C.-Y. Yuan, S.-J. Huang, H.-C. Huang, J. Sinkkonen, A. Oss, M.-L. Org, A. Samoson, H.-C. Tai, J. C. C. Chan, *Chem. Commun.* **2021**, *57*, 4110.

[24] T. Le Marchand, T. Schubeis, M. Bonaccorsi, P. Paluch, D. Lalli, A. J. Pell, L. B. Andreas, K. Jaudzems, J. Stanek, G. Pintacuda, *Chem. Rev.* **2022**, *122*, 9943.

[25] X. Lu, Y. Tsutsumi, C. Huang, W. Xu, S. R. Byrn, A. C. Templeton, A. V. Buevich, J.-P. Amoureux, Y. Su, *Phys. Chem. Chem. Phys.* **2020**, *22*, 13160.

[26] C. M. Quinn, R. Zadorozhnyi, J. Struppe, I. V. Sergeyev, A. M. Gronenborn, T. Polenova, *Anal. Chem.* **2021**, *93*, 13029.

[27] Y. Nishiyama, G. Hou, V. Agarwal, Y. Su, A. Ramamoorthy, *Chem. Rev.* **2023**, *123*, 918–988.

[28] P. Moutzouri, B. Simoes de Almeida, D. Torodii, L. Emsley, *J. Am. Chem. Soc.* **2021**, *143*, 9834.

[29] S. P. Brown, T. Schaller, U. P. Seelbach, F. Koziol, C. Ochsenfeld, F. G. Klarner, H. W. Spiess, *Angew. Chem. Int. Ed.* **2001**, *40*, 717; *Angew. Chem.* **2001**, *113*, 740.

[30] D. H. Brouwer, S. Alavi, J. A. Ripmeester, *Phys. Chem. Chem. Phys.* **2008**, *10*, 3857.

[31] P. Hodgkinson, *Prog. Nucl. Magn. Reson. Spectrosc.* **2020**, *118–119*, 10.

[32] P. Wikus, W. Frantz, R. Kümmerle, P. Vonlanthen, *Supercond. Sci. Technol.* **2022**, *35*, 033001.

[33] J. Wang, J.-M. Choi, A. S. Holehouse, H. O. Lee, X. Zhang, M. Jahnel, S. Maharana, R. Lemaitre, A. Pozniakovsky, D. Drechsel, I. Poser, R. V. Pappu, S. Alberti, A. A. Hyman, *Cell* **2018**, *174*, 688.

[34] S. Ullmann, R. Schnorr, C. Laube, B. Abel, B. Kersting, *Dalton Trans.* **2018**, *47*, 5801.

[35] Deposition Number 2168690 contains the supplementary crystallographic data for this paper. These data are provided free of charge by the joint Cambridge Crystallographic Data Centre and Fachinformationszentrum Karlsruhe Access Structures service.

[36] Deposition Number 2171903 contains the supplementary crystallographic data for this paper. These data are provided free of charge by the joint Cambridge Crystallographic Data Centre and Fachinformationszentrum Karlsruhe Access Structures service.

[37] J. C. Ma, D. A. Dougherty, *Chem. Rev.* **1997**, *97*, 1303.

[38] L. Liu, L. N. Zakharov, J. A. Golen, A. L. Rheingold, W. H. Watson, T. A. Hanna, *Inorg. Chem.* **2006**, *45*, 4247.

[39] D. Feller, *J. Phys. Chem. A* **1997**, *101*, 2723.

[40] J. D. Rodriguez, J. M. Lisy, *J. Am. Chem. Soc.* **2011**, *133*, 11136.

[41] A. Drljaca, M. J. Hardie, C. L. Raston, *J. Chem. Soc. Dalton Trans.* **1999**, 3639.

[42] M. Woińska, S. Grabowsky, P. M. Dominiak, K. Woźniak, D. Jayatilaka, *Sci. Adv.* **2016**, *2*, e1600192.

[43] C. Bannwarth, S. Ehlert, S. Grimme, *J. Chem. Theory Comput.* **2019**, *15*, 1652.

[44] S. Spicher, S. Grimme, *J. Chem. Theory Comput.* **2021**, *17*, 1701.

[45] D. C. M. Llunell, J. Cirera, P. Alemany, S. Alvarez, *SHAPE* **2013**, University of Barcelona.

[46] F. Glasneck, Q. I. Roode-Gutzmer, T. Stumpf, B. Kersting, *Chem. Eur. J.* **2022**, *28*, e202104301.

[47] A. J. Petrella, D. C. Craig, R. N. Lamb, C. L. Raston, N. K. Roberts, *Dalton Trans.* **2003**, 4590.

[48] B. Koeppe, P. M. Tolstoy, H.-H. Limbach, *J. Am. Chem. Soc.* **2011**, *133*, 7897.

[49] B. Koeppe, J. Guo, P. M. Tolstoy, G. S. Denisov, H.-H. Limbach, *J. Am. Chem. Soc.* **2013**, *135*, 7553.

[50] G. R. Fulmer, A. J. M. Miller, N. H. Sherden, H. E. Gottlieb, A. Nudelman, B. M. Stoltz, J. E. Bercaw, K. I. Goldberg, *Organometallics* **2010**, *29*, 2176.

[51] A. A. Malär, S. Smith-Penzel, G. M. Camenisch, T. Wiegand, A. Samoson, A. Bockmann, M. Ernst, B. H. Meier, *Phys. Chem. Chem. Phys.* **2019**, *21*, 18850.

[52] U. Sternberg, R. Witter, I. Kuprov, J. M. Lamley, A. Oss, J. R. Lewandowski, A. Samoson, *J. Magn. Reson.* **2018**, *291*, 32.

[53] M. P. Hanrahan, A. Venkatesh, S. L. Carnahan, J. L. Calahan, J. W. Lubach, E. J. Munson, A. J. Rossini, *Phys. Chem. Chem. Phys.* **2017**, *19*, 28153.

[54] G. Kervern, G. Pintacuda, Y. Zhang, E. Oldfield, C. Roukoss, E. Kuntz, E. Herdtweck, J.-M. Basset, S. Cadars, A. Lesage, C. Copéret, L. Emsley, *J. Am. Chem. Soc.* **2006**, *128*, 13545.

[55] A. Samoson, T. Tuherm, Z. Gan, *Solid State Nucl. Magn. Reson.* **2001**, *20*, 130.

[56] M. Alla, E. Lippmaa, *Chem. Phys. Lett.* **1982**, *87*, 30.

[57] J. C. Hindman, *J. Chem. Phys.* **1966**, *44*, 4582.

[58] A. Strate, V. Overbeck, V. Lehde, J. Neumann, A.-M. Bonsa, T. Niemann, D. Paschek, D. Michalik, R. Ludwig, *Phys. Chem. Chem. Phys.* **2018**, *20*, 5617.

[59] H. Eckert, Y. A. Levendis, R. C. Flagan, *J. Phys. Chem.* **1988**, *92*, 5011.

[60] J. Tabony, *Prog. Nucl. Magn. Reson. Spectrosc.* **1980**, *14*, 1.

[61] A. C. Forse, C. Merlet, C. P. Grey, J. M. Griffin, *Prog. Nucl. Magn. Reson. Spectrosc.* **2021**, *124–125*, 57.

[62] K. Saalwächter, F. Lange, K. Matyjaszewski, C.-F. Huang, R. Graf, *J. Magn. Reson.* **2011**, *212*, 204.

[63] T. Kobayashi, K. Mao, P. Paluch, A. Nowak-Król, J. Sniechowska, Y. Nishiyama, D. T. Gryko, M. J. Potrzebowski, M. Pruski, *Angew. Chem. Int. Ed.* **2013**, *52*, 14108; *Angew. Chem.* **2013**, *125*, 14358.

[64] B. Elena, L. Emsley, *J. Am. Chem. Soc.* **2005**, *127*, 9140.

[65] J. Kowalewski, L. Maler, *Nuclear Spin Relaxation in Liquids: Theory, Experiments, and Applications*, CRC, Boca Raton, **2006**.
[66] S. Macura, R. R. Ernst, *Mol. Phys.* **2002**, *100*, 135.
[67] V. Agarwal, *J. Magn. Reson.* **2020**, *311*, 106661.
[68] D. Suter, R. R. Ernst, *Phys. Rev. B* **1982**, *25*, 6038.
[69] S. Grimme, A. Hansen, S. Ehlert, J.-M. Mewes, *J. Chem. Phys.* **2021**, *154*, 064103.
[70] C. Adamo, V. Barone, *J. Chem. Phys.* **1999**, *110*, 6158.
[71] F. Jensen, *J. Chem. Theory Comput.* **2015**, *11*, 132.
[72] K. Raghavachari, G. W. Trucks, J. A. Pople, M. Head-Gordon, *Chem. Phys. Lett.* **1989**, *157*, 479.
[73] J. Gauss, J. F. Stanton, *J. Chem. Phys.* **1996**, *104*, 2574.
[74] M. Kállay, J. Gauss, *J. Chem. Phys.* **2004**, *120*, 6841.
[75] M. E. Harding, T. Metzroth, J. Gauss, A. A. Auer, *J. Chem. Theory Comput.* **2008**, *4*, 64.
[76] T. Kupka, C. Lim, *J. Phys. Chem. A* **2007**, *111*, 1927.
[77] T. Kupka, M. Stachów, M. Nieradka, J. Kaminsky, T. Pluta, *J. Chem. Theory Comput.* **2010**, *6*, 1580.
[78] T. Kupka, M. Stachów, M. Nieradka, J. Kaminsky, T. Pluta, S. P. A. Sauer, *Magn. Reson. Chem.* **2011**, *49*, 231.

Manuscript received: December 1, 2022
Accepted manuscript online: January 11, 2023
Version of record online: February 21, 2023